EXPERIMENTAL STUDY ON THE MECHANISM OF WATER AFFECTING THE PERMEABILITY CHARACTERISTICS OF SANDSTONE

by

Heng GAO[a], Zhi-Long ZHANG[a,b*], Jun LU[c], and Ze-Tian ZHANG[a,b,d]

[a]College of Water Resources and Hydropower, Sichuan University, Chengdu, China
[b]MOE Key Laboratory of Deep Earth Science and Engineering, Sichuan University, Chengdu, China
[c]Institute of Deep Earth Science and Green Energy, Shenzhen University, Shenzhen, China
[d]State Key Laboratory of Water Resource Protection and Utilization in Coal Mining, China Energy Investment Co. LTD, Beijing, China.

Original scientific paper
https://doi.org/10.2298/TSCI2301581G

The permeability characteristics of sandstone are of great importance for unconventional natural gas extraction, CO_2 geological storage, coal mine gas safety, etc. Under the influence of tectonic stress and mining-induced stress, the evolution of permeability becomes exceptionally complex. A number of studies have focused on the evolution of permeability under different stress paths, ignoring the effect of water on sandstone permeability. The permeability evolution of sandstone in dry and saturated states under high and low surrounding pressures was investigated by triaxial tests. The results show that the triaxial compressive strength of the specimen significantly decreases under saturated conditions. Specifically, the triaxial compressive strength decreases by 27.12% and 10.52% under low and high confining pressure, respectively. Compared to the dry specimen, the permeability of the saturated specimen significantly decreases at all stages of loading, the initial permeability of the saturated specimen is decreased by 92.09% and 56.25% at low and high confining pressure, respectively. The S&D model was matched with the test data, an excellent goodness of fit was obtained in the elastic and plastic phase, and the mechanism of water affecting sandstone permeability was analyzed.

Key words*: permeability evolution, sandstone, water, model matching*

Introduction

In the context of the increasing importance of unconventional gas extraction, it is important to study the permeability of sandstones. The study of sandstone is of great engineering significance for CO_2 geological storage, underground engineering construction, coal mine gas safety and unconventional natural gas extraction [1-7]. In recent years, against the backdrop of increasing attention to unconventional gas extraction, extensive research has been carried out by a large number of scholars on the permeability of reservoir rocks. Xie *et al*. [8]

*Corresponding author, e-mail: zzlxww@scu.edu.cn

conducted theoretical and experimental studies on the simultaneous exploitation of coal and gas to improve coal seam permeability, described the effect of mining on coal-rock permeability, and quantitatively captured the evolution of coal permeability. Li *et al*. [9] studied the permeability anisotropy of shale and developed a permeability model that can reflect the effect of each principal stress on permeability. Zhang *et al*. [10] and Xie *et al*. [11] conducted tests on coal containing natural fracture network distributions to investigate the relationship between effective pore space and stress; the permeability evolution was also studied under different mining methods [12]. Lu *et al*. [13, 14] studied the permeability and mechanical characteristics of layered composite coal-rock and proposed a permeability model for layered composite coal-rock. In unconventional natural gas extraction, the pores and throat channels are squeezed under the action of ground stress, making the seepage channels very narrow and poorly permeable or even impermeable, which is known from indoor tests. Thus, the problem of reservoir rock permeability is the key to natural gas extraction, which means that research related to the technology of increasing permeability, the law of permeability evolution and the factors affecting the permeability is crucial to oil and gas extraction [15].

The aforementioned study did not consider the effect of water on permeability. The limited pore throat space is the only channel for fluids, and water will occupy part of the seepage channel, which seems to be very unfavorable to permeability. In contrast, it is beneficial if the rock contains dissolved minerals such as clay, which may increase its permeability under the action of water, unblocking the originally closed pore throat or increasing the percolation channel. In practice, this situation is widespread in engineering; Groundwater and massive free water generated by hydraulic fracturing techniques and production can have a significant impact on permeability. The mechanism has yet to be investigated. Therefore, in this study, based on the above background, the permeability of sandstone under dry and saturated water contents is experimentally investigated under different surrounding pressures.

Experimental preparation

Testing apparatus and methods

The sandstone used in the experiment is from Shizhu County, Chongqing, Southwest China. A large block of sandstone with good homogeneity and no significant defects was selected. Cylindrical sandstone cores were drilled, and the specimens with a height-to-diameter ratio of 2:1, as recommended by the International Society for Rock Mechanics and Rock Engineering (ISRM). Moreover, it is guaranteed that the non-parallelism and non-perpendicularity are less than 0.05 mm.

The thermal-hydrological-mechanical coupling of coal (THM-2) apparatus developed independently by Chongqing University was used for testing. The device is mainly composed of a frame-type structure, a triaxial pressure chamber, a loading system, an inner sealing seepage system, a total control system, and a data measurement and acquisition system. In addition, the fluid is injected by a gas cylinder. The device can be used for the study of rock mechanical properties and permeability evolution laws under various stress path conditions, and it has high reliability and accuracy.

Since we temporarily disregarded the effect of temperature and the whole experiment was conducted at a constant temperature (the indoor temperature is 20 °C), the transport of CO_2 inside the sandstone can be regarded as a constant temperature laminar flow. This satisfies the basic conditions of Darcy's law [1, 16], and the expression used to calculate the permeability is suggested:

$$k = \frac{2P_0 Q \mu L}{A\left(P_1^2 - P_2^2\right)} \tag{1}$$

where k is the effective permeability, Q – the gas seepage flow, P_0 – the standard atmospheric pressure (about 0.1 MPa), μ – the CO_2 gas dynamic viscosity (we take $1.4932 \cdot 10^{-11}$ MPa s), L – the length of the specimen, P_1 – the inlet gas pressure (1.5 MPa), P_2 – the outlet gas pressure (0.1 MPa), and A – the effective area of gas seepage. More general case for the Darcy's law was suggested in [17].

Experimental results and analysis

Stress and strain characteristics of sandstone

As shown in fig. 1, the full stress–strain curves of sandstone specimens under different conditions showed the same properties. The specimens were axially compressed as positive strain and radially expanded as negative strain, and the volume strain was positive before damage and expanded after damage. The difference is that the triaxial strength increases with increasing confining pressure for both dry and saturated specimens. The strength of the specimens in the saturated state is always much lower than that in the dry state at the same confining pressure. The triaxial compressive strength decreased by 27.12% in the low confining pressure ($\sigma_2 = \sigma_3 = 5$ MPa) test, and the triaxial compressive strength decreased by 10.52% in the high confining pressure ($\sigma_2 = \sigma_3 = 25$ MPa) test. The reason may be that water dissolves the soluble minerals such as clay in the sandstone, which leads to a weakening of the skeletal structure of the porous material and, in turn, decreases the strength of the specimen.

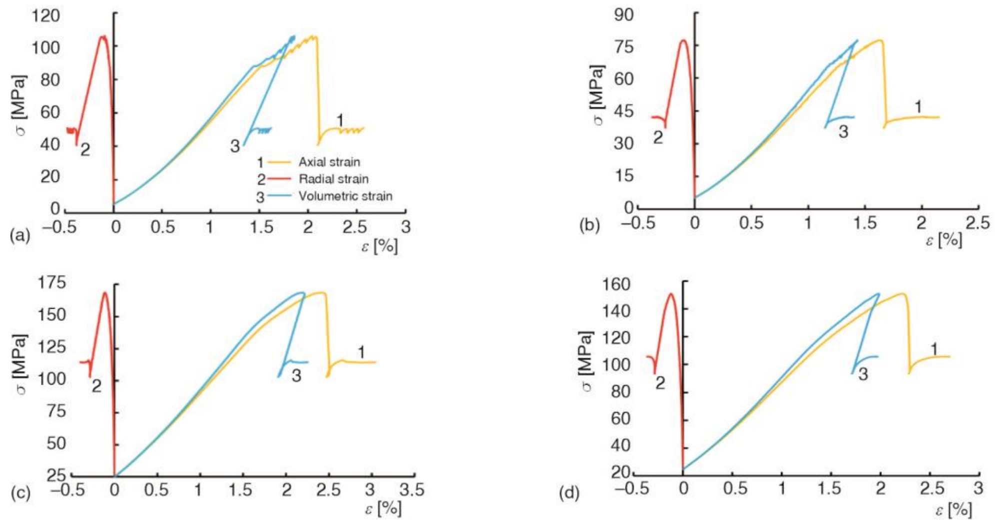

Figure 1. The full stress–strain curves of sandstone specimens under different conditions; (a) SSL5D, (b) SSL5S, (c) SSL25D, and (d) SSL25S

It is worth pointing out that the elastic modulus (σ/ε) changes abruptly (decreases) when the specimen transforms into the plastic phase at low confining pressure, while at high confining pressure, the elastic phase transforms into the plastic phase with a gradual change in the elastic modulus, and the stress–strain curve is very smooth, as shown in fig. 1. This indicates that a certain size of the confining pressure is beneficial for maintaining the strength of the rock, which is important in engineering practice.

Full range of permeability evolution characteristics

Under lower confining pressure test conditions, the variation in axial stress, radial strain, volumetric strain and permeability throughout the test is illustrated in fig. 2. For the dry sandstone specimen test (SSL5D), it can be observed from the figure that there is a good correspondence among stress, strain and permeability. At the beginning of loading, the axial stress increases slowly, the specimen is compressed uniformly in the axial direction, the volume gradually decreases, a relatively small negative strain is generated in the radial direction, and the permeability then gradually decreases (decreased by 20.14%). In the pore compacting stage and elastic deformation stage, as the pore throat space is squeezed, the skeletal medium occupies more space, which decreases the permeability. When entering the plastic stage, the radial deformation gradually increases, and the permeability also gradually increases. Eventually, the specimen is damaged, and a large crack is formed, which leads to an instantaneous increase in permeability. It is shown that the process of slowly expanding cracks gradually generates new permeability channels (microcracks).

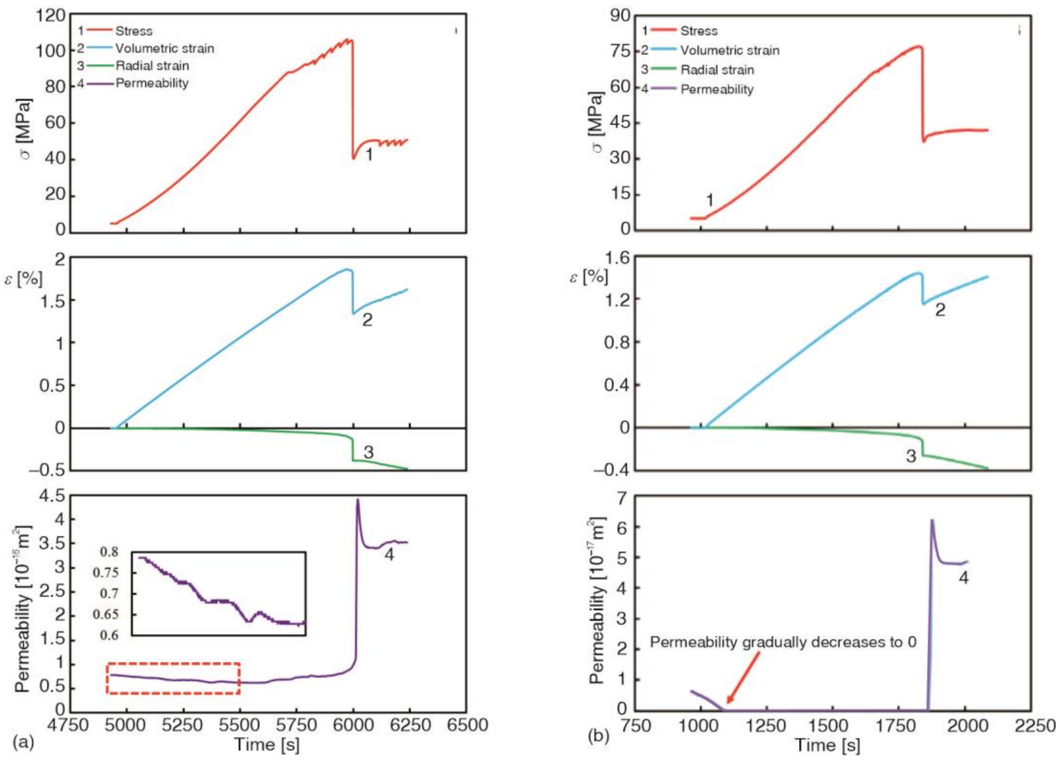

Figure 2. Evolution characteristics of stress–strain–permeability under low confining pressure; (a) SSL5D and (b) SSL5S

In the saturated sandstone specimen test (SSL5S), it is clearly observed that the initial permeability k_0 is smaller than that of dry sandstone. Compared to the dry specimen, the initial permeability of the saturated specimen is decreased by 92.09%, and with axial loading, the permeability quickly decreases to 0. At this time, the specimen is no longer permeable at the tested permeability pressure (1.5 MPa). The specimen did not regain permeability until damage occurred and macroscopic cracks were produced. The cracks produced by the damage became new percolation channels, and permeability grew by almost an order of magnitude as the cracks penetrated the specimen. The results indicate that the pore throats of the sandstone were clogged by water, making it impossible for the gas to flow. Additionally, it can be seen in the figure that the sandstone with saturated water content loses permeability much faster than the dry rock when loaded by axial forces. It can be concluded that the water-rock coupling state makes it more difficult for the gas to be transported in the porous media.

Furthermore, compared to low perimeter pressure test conditions, the permeability under high confining pressure conditions is lower by an order of magnitude. In the case of dry sandstone (SSL25D), the permeability decreased by 18.75% in the pore compression stage and elastic stage, and gradually increased in the plastic stage with the generation of microcracks. After damage to the specimen, the permeability far exceeds the initial value. As show in fig. 3.

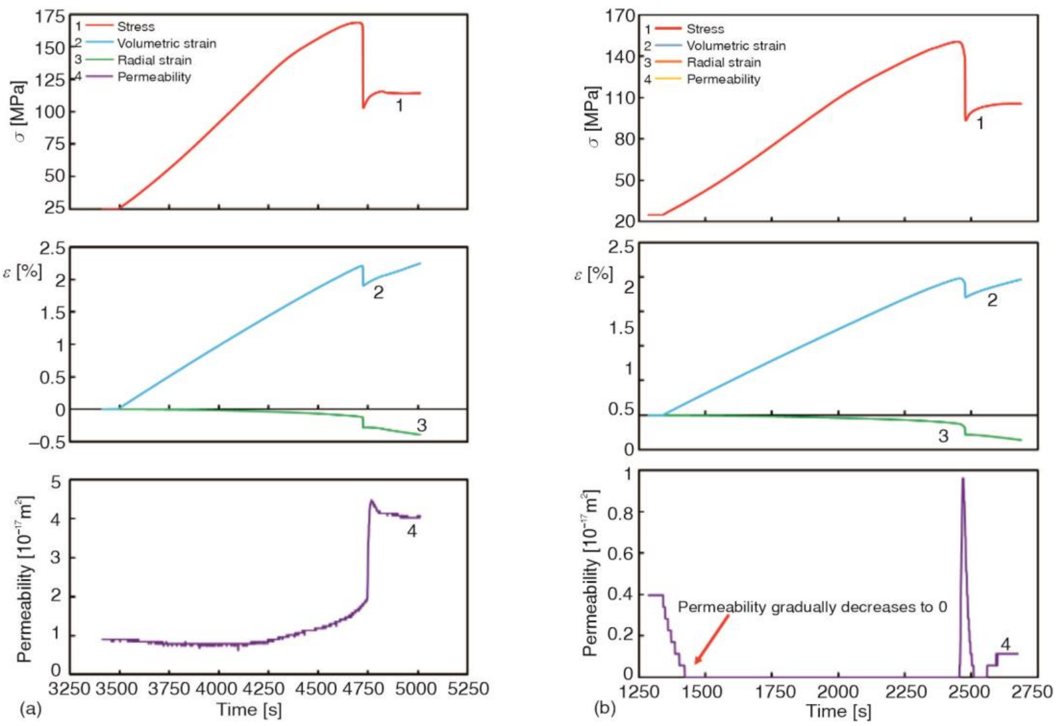

Figure 3. Evolution characteristics of stress–strain–permeability under high confining pressure; (a) SSL25D and (b) SSL25S

In the saturated water test (SSL25S), the initial permeability is extremely low but still of the same order of magnitude as the dry specimen test. The initial permeability is reduced by 56.25% and then quickly drops to zero with axial loading. At the time of damage to the specimen, although there was an increase in the permeability, this increase was not significant compared to the test case with a low confining pressure. In addition, there was not a gradual increase in the permeability in the plastic stage. The reason for this is that the micro-cracks created in the plastic stage were not sufficient for gas transport under the action of water. In other words, the micro-crack channels were occupied by water.

Discussion

In this section, the permeability evolution pattern of dry and saturated water sandstones in axially loaded tests is discussed. Therefore, the permeability model shown in eq. (2) is included in the scope repertoire of the discussion. It is known as the S&D model is given [1]:

$$k = k_0 e^{-3C_f(\sigma_1 - \sigma_{1\text{-}0})} \tag{2}$$

where C_f is the cleat volume compressibility, σ_1 – the axial stress, and σ_{1-0} – the initial stress.

In eq. (2), the cleat volume compressibility was extended to the fracture compressibility, and the fracture compressibility C_f is described as a constant in this model. Existing studies, however, have found that fracture compressibility is not constant but changes with varying stress conditions [1]. The permeability of sandstone specimens progressed through elastic and plastic stages, with the permeability decreasing and then increasing. The reason for the decrease in permeability in the elastic stage is due to the extrusion of the pore throat, and the reason for the increase in permeability in the plastic stage is due to the expansion of cracks, and the value of C_f is changed. In simple terms, fracture compressibility is a function of stress:

$$k = k_0 \mathrm{e}^{-3\overline{C_f}(\sigma_1 - \sigma_{1\text{-}0})}, \ \overline{C_f} = \frac{C_{f0}}{\alpha(\sigma_1 - \sigma_{1\text{-}0})}[1 - \mathrm{e}^{-\alpha(\sigma_1 - \sigma_{1\text{-}0})}] \tag{3}$$

where $\overline{C_f}$ is the mean equivalent fracture compressibility, C_{f0} – the initial equivalent fracture compressibility and α is the declining rate of equivalent fracture compressibility with increasing stress.

The permeability-stress curves contain elastic, plastic and postpeak phases. The postpeak stage of the specimen was damaged, and macroscopic large cracks were produced. It remains to be further investigated whether Darcy's law still applies. Therefore, the postpeak stage of permeability is not in the scope of discussion. The test data were divided into two parts, decreasing penetration and increasing penetration with increasing axial stress, and were matched to the S&D model.

The fitting results of the dry specimens are shown in fig. 4, excellent goodness of fit values were obtained for the different confining pressure conditions. The coefficient of determination, R^2, is 0.9797 and 0.9038 in the elastic and plastic stages at low confining pressures, respectively, and the R^2 is 0.9635 and 0.9801 in the elastic and plastic stages at high confining pressures, respectively. We can see that the initial equivalent fracture compressibility, C_{f0}, and the declining rate of equivalent fracture compressibility, α, are positive in the elastic stage and negative in the plastic stage, which reflects the mechanism of permeability evolution. That is, the pore throat is squeezed in the elastic section, the seepage channel becomes narrower, and this squeezing process becomes increasingly difficult; in other words, this compressibility shows a weakening trend. In the plastic section, the crack sprouts, increasing the fluid circulation space, and this tendency of increasing seepage channels gradually increases.

The fitting results for the saturated specimens are shown in fig. 5, and all specimens similarly obtained excellent goodness of fit values under different circumferential pressure conditions. The R^2 is 0.9797 and 0.9887 for the elastic phase at low and high confining pressures, respectively. It should be noted that under saturated specimen test conditions, the specimen exhibits no permeability in the plastic phase (before damage) under the action of water. For that reason, we could not obtain enough data to characterize the permeability evolution during crack expansion. Therefore, the plastic phase in the saturated state is temporarily left out of the fitting process. Combining the fitting results of fig. 4, fig. 5, and tab. 1, it can be seen that the effect of water makes α change from positive to negative. As the axial stress increases, $\partial\overline{C_f}/\partial\sigma$ increases. This indicates that the action of water makes the permeability decrease faster and the stress sensitivity is more intense. There is:

$$\frac{\partial\overline{C_f}}{\partial\sigma}=-\frac{C_{f0}}{\alpha\sigma^2}(1-\mathrm{e}^{-\alpha\sigma})+\frac{C_{f0}}{\sigma}\mathrm{e}^{-\alpha\sigma} \tag{4}$$

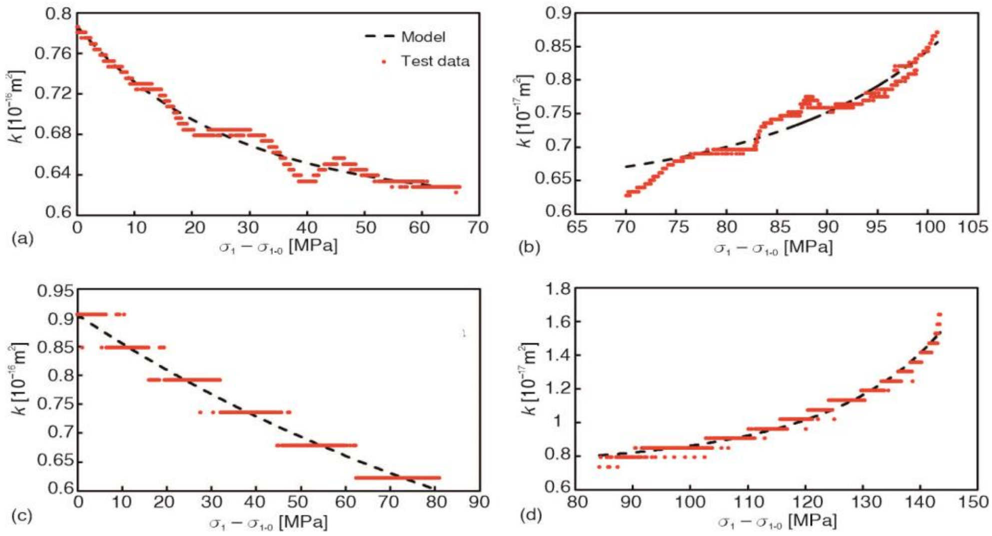

Figure 4. Comparison of experimental data (dry sandstone) with the S&D model; (a) elastic phase of SSL5D, (b) plastic phase of SSL5D, (c) elastic phase of SSL25D, and (d) plastic phase of SSL25D

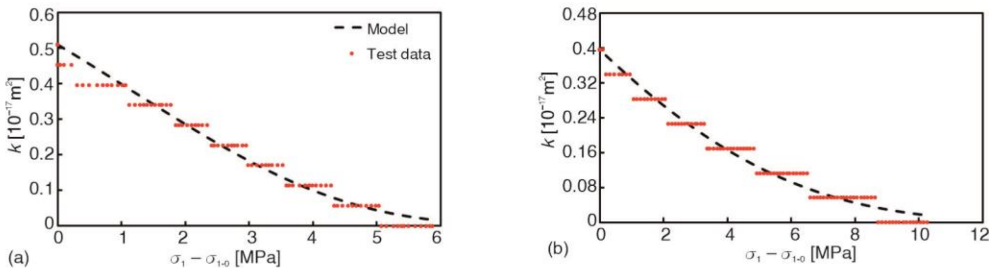

Figure 5. Comparison of experimental data (saturated sandstone) with the S&D model; (a) plastic phase of SSL5S and (b) plastic phase of SSL25S

Table 1 Best fitting parameters for experimental data

Specimen number	Fitting result			Specimen number	Fitting result	
	Parameters	Elastic stage	Plastic stage		Parameters	Elastic stage
SSL5D	C_{f0}	0.0028	–3.5320	SSL5S	C_{f0}	0.0703
	α	0.0332	–0.0493		α	–0.2993
	R^2	0.9797	0.9038		R^2	0.9774
SSL25D	C_{f0}	0.0019	–5.7411	SSL25S	C_{f0}	0.0586
	α	0.0032	–0.0349		α	–0.1013
	R^2	0.9635	0.9801		R^2	0.9887

Conclusion

The self-developed THM-2 system was used for testing, and dry and saturated sandstones were subjected to permeability testing at high and low confining pressures. The role of water in the transport of CO_2 in sandstone was investigated. The presence of water significantly reduces the permeability of the sandstone. Compared to the dry specimen, the permeability of the saturated specimen is decreased by 92.09% in the low confining pressure test, and the permeability is reduced by 56.25% in the high confining pressure test. Both dry and saturated sandstones conform to the evolution law described by the S&D model, and the test data fit well with the model. The mechanism by which water decreases sandstone permeability is as follows. At the physical level, the mechanism is influenced by the presence of water, which occupies the pore throat and makes it more difficult to transport gas. At the theoretical model level, the effect of water makes the value of α become negative, which makes the rate of change in C_f greater; that is, the sensitivity of sandstone increases

Acknowledgment

The Open Fund of State Key Laboratory of Water Resource Protection and Utilization in Coal Mining (Grant No. SHJT-17-42.13), National Natural Science Foundation of China (Grant No. 52104209) and the Postdoctoral Research Foundation of China (Grant No. 2021M692192).

Nomenclature

A – effective area of gas seepage, [m^2]
C_f – cleat volume compressibility, [–]
C_{f0} – initial equivalent fracture compressibility, [–]
$\overline{C_f}$ – declining rate of equivalent fracture compressibility, [–]
k – effective permeability, [m^2]
Q – gas seepage flow, [m^3s^{-1}]

Greek symbols

α – mean equivalent fracture compressibility, [–]
σ_1 – axial stress, [MPa]
$\sigma_{1\text{-}0}$ – initial stress, [MPa]
μ – CO_2 gas dynamic viscosity, [MPa s]

References

[1] Gao, H., *et al.*, Experimental Study on Influence of Intermediate Principal Stress on the Permeability of Sandstone, *Transport in Porous Media*, *135* (2020), 3, pp. 753-778
[2] Zhang, Z. T., *et al.*, An Anisotropic Coal Permeability Model that Considers Mining-Induced Stress Evolution, Microfracture Propagation and Gas Sorption-desorption Effects, *Journal of Natural Gas Science and Engineering*, *46* (2017), 10, pp. 664-679
[3] Xie, J., *et al.*, Experimental Investigation on the Gas Flow Characteristics of Coal Samples with Different Fracture Network Complexities, *Journal of Natural Gas Science and Engineering*, *82* (2020), Oct., 103487
[4] Ai, T., *et al.*, Changes in the Structure and Mechanical Properties of a Typical Coal Induced by Water Immersion, *International Journal of Rock Mechanics and Mining Sciences*, *138* (2021), Feb., 104597
[5] Lu, J., *et al.*, Mechanical Properties and Failure Mode of Sandstone Specimen With a Prefabricated Borehole Under True Triaxial Stress Condition, *Geomechanics for Energy and the Environment*, *25* (2020), Mar., 100207
[6] Zhang, Z. P., *et al.*, Deformation Damage and Energy Evolution Characteristics of Coal at Different Depths, *Rock Mechanics and Rock Engineering*, *52* (2019), 5, pp. 1491-1503
[7] Zhang, A. L., *et al.*, Mechanical Properties and Energy Characteristics of Coal at Different Depths Under Cyclic Triaxial Loading and Unloading, *International Journal of Rock Mechanics and Mining Sciences*, *161* (2023), Jan., 105271
[8] Xie, H. P., *et al.*, Theoretical and Experimental Validation of Mining-Enhanced Permeability for Simultaneous Exploitation of Coal and Gas, *Environmental Earth Sciences*, *73* (2015), 10, pp. 5951-5962

[9] Li, M. H., *et al.*, Permeability Evolution of Shale Under Anisotropic True Triaxial Stress Conditions, *International Journal of Coal Geology*, *165* (2016), Aug., pp. 142-148
[10] Zhang, Z. T., *et al.*, The Relationships among Stress, Effective Porosity and Permeability of Coal Considering the Distribution of Natural Fractures: Theoretical and Experimental Analyses, *Environmental Earth Sciences*, *73* (2015), 10, pp. 5997-6007
[11] Xie, H. P., *et al.*, Stress-Fracture-Seepage Field Behavior of Coal Under Different Mining Layouts, *Journal of China Coal Society*, *41* (2016), 10, pp. 2405-2417
[12] Zhang Z. T., *et al.*, Mining-Induced Coal Permeability Change Under Different Mining Layouts, *Rock Mechanics and Rock Engineering*, *49* (2016), May, pp. 3753-3768
[13] Lu, J., *et al.*, Permeability Characteristics of Layered Composite Coal-Rock Under True Triaxial Stress Conditions, *Journal of Natural Gas Science and Engineering*, *66* (2019), June, pp. 60-76
[14] Lu, J., *et al.*, Mechanical Properties of Layered Composite Coal–Rock Subjected to True Triaxial Stress, *Rock Mechanics and Rock Engineering*, *53* (2020), 9, pp. 4117-4138
[15] Liu, M., *et al.*, Characterization of Pore Structures of Tight Sandstone Reservoirs by Multifractal Analysis of the NMR T2 Distribution, *Energy Fuels*, *32* (2018), 12, pp. 12218-12230
[16] Lu, J., *et al.*, Deformation and CO_2 Gas Permeability Response of Sandstone to Mean and Deviatoric Stress Variations Under True Triaxial Stress Conditions, *Tunnelling and underground space technology*, *84* (2019), Feb., pp. 259-272
[17] Yang, X.-J., New Insight Into the Fourier-Like and Darcy-Like Models in Porous Medium, *Thermal Science*, *24* (2020), 6A, pp. 3847-3858

Paper submitted: August 7, 2022
Paper revised: November 12, 2022
Paper accepted: November 22, 2022